Preprints of the 19th World Congress
The International Federation of Automatic Control
Cape Town, South Africa. August 24-29, 2014

Acoustic Emission, a New Sensor for Monitoring Industrial Crystallization Processes

Gilles Fevotte*[⌖], XingJun Wang[❄]*, Yamina Ouabbas*

* Ecole Nationale Supérieure des Mines, SPIN, F-42023 Saint-Etienne, 158 cours Fauriel, France.
Contact email : fevotte@univ-lyon1.fr
[⌖] Université Claude Bernard Lyon 1, Université Lyon 1, 43 bd du 11 Novembre 1918. 69622 Villeurbanne. Cedex. France.
[❄] Qiannan Normal College for Nationalities, Department of Physics, LongShan Road, 558000 Duyun, P.R.China

Abstract: The potential of Acoustic Emission (AE) for monitoring industrial crystallization processes is investigated through the monitoring of two typical crystallization systems. The sensing technology is successfully applied to monitoring the batch cooling solution crystallization of Citric Acid (CA) in water, which exhibits a anhydrous to monohydrate phase transition. The technique is also applied to monitoring the precipitation of salicylic acid from its sodium salt. A huge amount of acoustic data is recorded by the AE system, and the analysis of this data set is focused on the evaluation of AE as a new sensor for monitoring the basic steps of the crystallization process (i.e., nucleation, growth, phase transition, etc.) A time- and frequency domain analysis is presented which shows the wealth of the technique. It is finally concluded that AE allows a very early detection of nucleation events, provides a means of monitoring the development of the crystallization or precipitation process and allows monitoring solvent-mediated phase transition phenomena occurring under cooling. It is thus suggested that acoustic emission could be valuable in the development of new crystallization monitoring and control strategies: this is all the more interesting that the acoustic piezo-sensor is non-intrusive and does not require any sampling of the slurry, two features which are of tremendous importance in the field of cooling crystallization processes.

Keywords: Monitoring, sensors, industrial crystallization, batch control, data processing, acoustic emission.

1. INTRODUCTION

One means of improving the quality of industrial particulate products is to design and apply efficient control strategies. To do this, sensors should be made available for monitoring in real time the development of the transformation phenomena involved during the solid generation and for applying corrective actions(Larsen and Rawlings, 2009, Nagy et Braatz, 2012). During the past 20 years, many hopes have been placed in the development of the so-called "Process Analytical Technologies" (PATs) (see e.g. Yu et al., 2004). Significant technological advancements have indeed been made that allowed developing new advanced sensing strategies. Even though they do not solve all problems raised by the monitoring of particulate processes, these technological advancements enabled the possibility of exploiting more in depth, relevant, reliable and frequent process data.

Technologies required for monitoring and control particulate processes should essentially be focused on three aspects of the solid production process. Firstly, information about the concentrations (taken in a wide sense) of the products should be made available. This is typically the case, for example, with solution crystallization systems were the solute concentration allows computing supersaturation, the driving force of crystallization (Févotte, 2002). Secondly, for obvious reasons, any information related to the dispersed phase is of tremendous interest for improving the mastery over the development of the process and improving the quality of the obtained particles (e.g., the size of crystals, their moisture content, the state of agglomeration, the crystal shapes, etc.) Thirdly, gaining any "real-time" information related to the end-use quality features of the final product is obviously of great interest for better mastering the quality of particulate products.

As far as particulate processes are concerned, developing new sensing and monitoring strategies is still an open problem because desirable measurement devices are simply lacking or provide insufficient and/or problematic information. For example, despite its wide industrial use, the FBRM probe cannot be considered as a "true" CSD sensor since it only measures chord length distributions (CLD). Depending on the shape and on the optical properties of the particles, the CLD is likely to provide a very poor representation of the CSD. This is why it is rather hazardous to use the CLD data for control purposes without precautions. Moreover, most modern devices suitable for monitoring particulate processes are still rather sophisticated and costly, and usually require complex and time-consuming calibration procedures. It should also be outlined that most PAT sensors are set in situ: this raises significant practical difficulties.

Acoustic emission (AE) has been widely used in the past as a non-destructive sensing technique in many fields of manufacturing processes (Bouchard, Payne and Szyszko 1994; Burnett, 2011) AE is today a sensing tool of choice in the steel industry, aeronautics, building industry, automotive industry, etc. (Jayakumar et al., 2005). As far as process engineering is concerned, AE has been applied to a variety of real time process monitoring applications even though, to the best of our knowledge, it was rarely envisaged in the high value added chemistry process industry. Few studies focused on the AE monitoring of chemical engineering processes were reported, including fluidized bed granulation(Briongos et al. 2013), fluidized bed coating (Naelapää, K. *et al.*, 2007), drying, powder compaction, grinding (Aguiar *et al*. 2004), but almost none of these studies dealt with the AE monitoring of solution crystallization processes.

2. ACOUSTIC EMISSION

2.1 Basic Principle

The technique of AE uses a transducer coupled to a process in which various materials are undergoing dynamic mechanical changes (Burnett, 2011; Grosse et Ohtsu, 2008). The sensor detects the elastic energy of acoustic waves propagating from the physical source of emission. The latter can arise from many mechanical or physical phenomena like fracture, plastic deformation, phase transition, delamination, etc.) During a given process, multiple physical sources can therefore generate AE. This is why acoustic signals present intricate and diversified waves and emission frequency spectra are generally complex. However, one can reasonably expect that, depending on the physical phenomena of interest, relevant information can be extracted and correlated to the development of the process under monitoring.

A major advantage of the AE technique lies in its non-intrusive features: piezo-sensors do not need to be placed inside the process medium (e.g., dryers, granulators, grinders, crystallizers, etc.) The technology can therefore be used in hard process conditions including high temperature and/or high pressure conditions, highly corrosive media and outside environments where the growth of pathogenic organisms can take place. Another advantage of AE lies in the possibility of collecting a wide range of information in real-time. As far as crystallization systems are concerned, one can thus expect AE to allow approaches for gaining a new viewpoint on basic crystallization phenomena (e.g., nucleation, growth, agglomeration …), to increase process understanding and provide a basis for innovative online control applications. When crystal particles are generated, the elastic properties of the dispersed phase change. Inter-particles and/or particles-wall frictions can also occur and generate size-dependent acoustic emission. Other particle properties such as shape, hardness or brittleness can also affect the elasticity of the dispersed phase and its kinetic energy.

Evaluating the potential for using acoustic emission during batch solution crystallization processes is therefore of great interest. In particular, the ability of the AE technology in detecting specific event such as nucleation phenomena or phase transition deserves to be assessed.

2.2 The equipment of acoustic emission.

The AE device consists of a piezo-electric sensor fixed on the wall of the equipment where the process occurs. Coupling grease is used to improve the transmission of acoustic waves from the emitting medium (i.e., particle bed or particle suspension) to the acoustic sensor, through the wall of the equipment (see Fig.2). AE signals produced by physical events such as breakage, inter-particle collisions or compression, are transmitted from their physical source to the sensor where they are converted into an electronic signal, which is then conditioned, amplified, filtered and processed by specific fast Data Acquisition System connected to the probe.

2.3 Some features of AE signals.

The acoustic emission can be considered as a sequence of "hits" which are described in Fig. 1. In order to differentiate significant hits from noise, a reference level of energy (about 600 atto-Joules, with 1 aJ=10^{-18} J) and a threshold power ratio value (e.g. 30 dB) should first be determined from "blank" measurements performed to get rid of insignificant signals emitted by the electromagnetic environment or the equipment itself. AE parameters related to the energy of AE waves, features of bursts (e.g., the number of counts and amplitude) or frequency characteristics of waves can be recorded.

Rather than processing the many raw acoustic signals, global AE parameters can be computed to avoid storing too large a number of data. For example, as displayed in Fig. 1, a given acoustic burst can be characterized by the duration of the burst or its maximum amplitude, after integrating the output signal exceeding a given threshold, or after computing its average and/or the number of counts *n*. Such global parameters are called descriptors. It is clear that working with descriptors is easier than working with the whole raw pseudo-periodic data. The use of descriptors is also less CPU-time consuming because they can be processed without manipulating excessive amounts of data.

For example, a basic parameter used to characterize the level of acoustic signals in the time domain is the root mean square value (RMS) defined as follows:

$$\bar{p}_{rms} = \sqrt{\frac{1}{t_2 - t_1}} \int_{t_1}^{t_2} p(t)^2 \, dt \qquad (1)$$

where $p(t)$ is the pressure magnitude of a continuous acoustic wave taken between times t_1 and t_2.

From a practical point of view, and as displayed in Fig.1, $p(t)$ is evaluated as an electrical voltage $u(t)$ emitted by the acoustic transducer and amplified by the sensing device, such that: $u(t) \propto p(t)$.

The amplitude of a given hit is the maximal voltage of the AE signal divided by the reference voltage of the sensor (of the order of 1 μV). The average frequency $\bar{f}$ is defined as the average ratio between the number of counts *n* and the duration of the burst. The peak frequency, expressed in kHz,

is defined as the point in the power spectrum at which the peak magnitude is observed, and the frequency centroid $\tilde{f}$ is the barycentre computed from the sum of the frequencies balanced by the magnitude of the wave, it is thus equivalent to a first moment of inertia. The absolute energy, in atto-Joule (1 aJ=10^{-18} J) is defined from the integration of the output voltage *u(t)* of the transducer, α being inversely proportional to the electrical resistance of the measuring circuit:

$$E_{abs} = \alpha \int u(t)^2 \, dt \qquad (2)$$

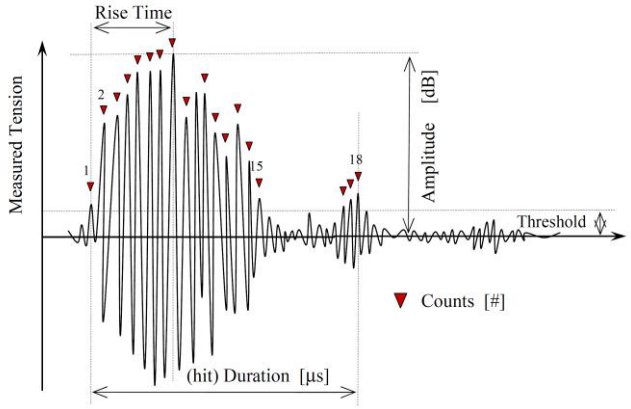

Fig. 1. Typical acoustic burst and main related descriptors.

2.4 Crystallization setup.

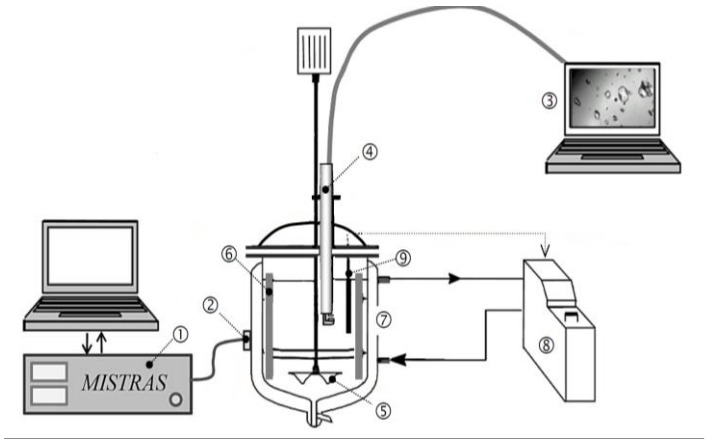

Fig. 2: Experimental set-up: temperature controlled well-mixed batch crystallizer equipped with acoustic emission piezo sensor (2). (1) Acoustic data acquisition system, (3) Computer dedicated to in situ image acquisition and processing, (5) Mixing propeller, (6) Baffles, (7) Cooling jacket, (8) Heating/cooling bath, (9) Temperature probe.

A schematic of the crystallization setup used during the present study is displayed in Fig.2. Batch cooling experiments were performed using this equipment. The slope of the decreasing linear setpoint trajectory was set constant, which did not help the cooling process to deviate from its set point trajectory in the presence of significant thermic effects. As one can see in Fig.3, the crystallization was initiated during cooling thanks to the introduction of small amounts of anhydrous or monohydrate citric acid seed particles (less than 0.1 wt %) at a temperature depending on the desired initial polymorphic state (i.e., anhydrous or monohydrate) and on the initial solute concentration. Seed was used to master the starting of the crystallization process and the phase of the crystallizing solid without avoiding secondary nucleation. The state of the seed was checked using Raman spectroscopy.

The experiments were performed in a 3 L glass vessel equipped with a jacket and a high efficiency propeller. The bench-scale plant was instrumented and computer-controlled. More details about the overall experimental design can be found in (Gherras *et al*., 2012)

3. A FIRST MODEL SYSTEM: CRYSTALLIZATION OF CITRIC ACID IN WATER;

3.1 Solubility diagram

Citric acid can crystallize in water as anhydrous or monohydrate between 0°C and 60°C. The two solid forms are referred to as CAa and CAm in the following. The crystallization experiments were performed in distilled water. CAa was initially dissolved in water with a concentration of 2.9 kg anhydrous/kg water. Fig. 3 displays the corresponding solubility curves. The initial concentration corresponds to a saturation temperature of about 65°C. CAa is more stable above the transition point located closed to 35°C, while CAm is more stable below (for more details see Caillet *et al.*, 2007; Caillet, Sheibat-Othman *et al,* 2007).

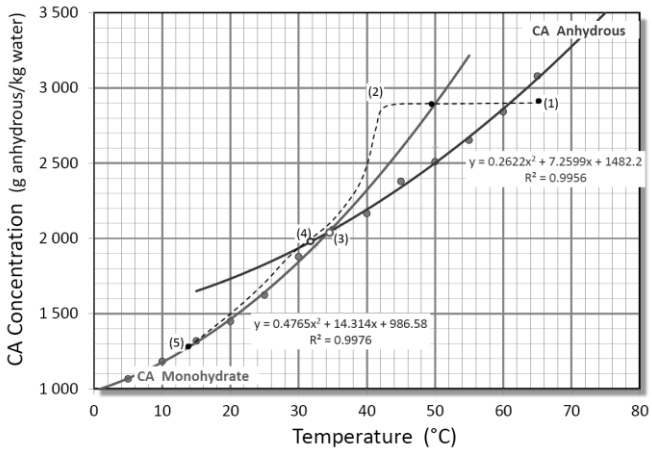

Fig. 3. Solubility diagram of citric acid in water. (1) Initial undersaturated solution; (2) Seeding with CAa; (3) Transition point (35°C); (4) Solvent-mediated phase transition (The solubility curve of CAa is crossed around 32°C); (5) End of the crystallization of CAm.

3.2 Experimental procedure

Cooling crystallization experiments were carried out as described above with a constant setpoint cooling rate dT/dt=-15°C/h. The temperature evolved from T = 59°C to 15°C.

The ability of AE to detect secondary nucleation phenomena induced through seeding was first evaluated. Due to the poor

heat transfer capacity of the glass wall of the jacket, the linear target temperature trajectory could not be met when significant exothermal processes occurred during the batch process. The linearity of the temperature profile was thus lost when massive crystallization took place. The cooling batch crystallization of citric acid can gave rise to anhydrous to monohydrate solvent mediated phase transition. From this point of view the recorded temperature trajectory (not shown here) clearly exhibited two temperature bumps related to the successive crystallization of anhydrous and monohydrate CA during the cooling process.

The sequence of the acoustic waves turned out to be almost continuous. In other words, it was rather difficult to isolate separate bursts (i.e. like the one displayed in Fig. 1) from the oscillatory AE signal. This is the reason why the tuning parameters allowing distinguishing between two successive bursts had to be carefully tuned, prior to any relevant acquisition and computation of the descriptors.

3.3 Experimental results

To give an idea of the development of crystallization operation during which anhydrous to monohydrate phase transition, a qualitative trajectory of the concentration of citric acid is plotted in Fig. 3. Consistently with the concentration trajectory of citric acid, two exothermal effects were observed which are related to the 2 successive crystallization processes involved during the batch cooling operation. These effects correspond to points (2) and (4) in Fig.3.

During the temperature evolution between 65°C and 49°C, no significant acoustic activity was detected, as one can see in Fig.4 which represents the time vs. peak frequency dots corresponding to every detected single acoustic burst. This initial batch period is referred to as "period α" in Fig.4. Between 49°C and 40°C, the nucleation of the anhydrous form of citric acid is expected to take place and should be considered together with the acoustic activity displayed in Fig.4. The latter figure shows that most of the acoustic activity occurs during this time interval referred to as "period β". Period γ follows during which the acoustic activity above 150 kHz has almost disappeared. This period corresponds to the end of the crystallization of CAa, it is followed by period δ during which CAa dissolves in favour of the nucleation and growth of the CAm crystal form.

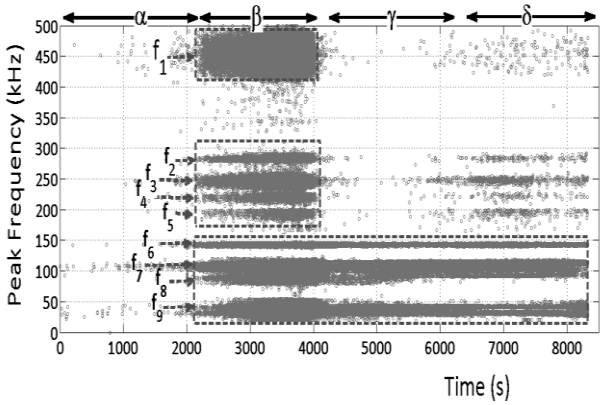

Fig.4. Time plot of the individual peak frequencies during the crystallization of citric acid. Dashed boxes outline main frequency bands

3.4 Discussion of the results

A scenario for the crystallization process with solvent-mediated phase transition is now proposed to support a possible explanation of the acoustic activity. Fig.5 is presented to make the comparison between the various experimental results easier. A first difficulty raised by these results is the unexpected shift between "period β" and the experimental temperature profile. The onset of the acoustic activity takes place around t_1 =2000 s (even a little bit earlier) while the temperature increase associated with the development of anhydrous crystallization starts around t=3300 s. Visual observation of the crystallizing slurry shows that many crystals are in fact generated during period β: it makes no doubt (see Fig. 3) that the highest level of supersaturation and, consequently, the highest nucleation rates are occurring during the same period. Now, during period γ, as already outlined, frequency bands f_1 to f_5 (see Fig.4) are no more active (i.e., crystal growth now dominates the overall crystallization process), while the remaining supersaturation – with respect to the anhydrous from of CA – is still positive. It seems therefore reasonable to assume that bands f_1 to f_5 could be indicative of the nucleation process. This latter assumption is consistent with the fact that bands f_6 to f_9 can be observed during the whole batch duration. Crystal growth is indeed the only permanent basic crystallization process from time t_1 to the end of cooling.

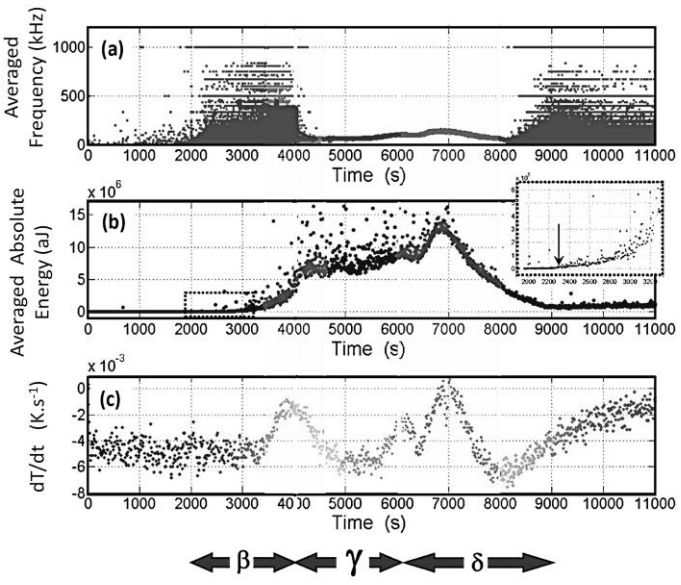

Fig.5. Comparison between the thermal effect of the development of the crystallization process (curve c) and both frequency and absolute energy of the acoustic waves. Time periods α to δ refer to Fig.4.

Fig.5 compares the development of the thermal effect of crystallization with the time variations of both the average frequency and the average absolute energy. Displaying the whole set of absolute energy data (see e.g. the dots in Figure 6) would lack of clarity and, anyway, could not give a clear

idea of the overall trends of the distribution of AE energy. This is why the absolute energy of the acoustic events was averaged as follows, where N_k is the total number of hits recorded during sample n°k, the sampling period being 3 seconds:

$$\overline{E}_{abs,k} = \frac{\sum_{k=1}^{N_{i,j}} E_{abs}(k)}{N_k} \quad (3)$$

$\overline{E}_{abs,k}$ is plotted in Fig.5b, the plot shows that the acoustic activity becomes significant at the approximate time of 2250s. (see the insert) The same processing was made with the frequency data. The results are plotted in Fig.5a.

Now, one could object that stirring, through inter-particles and particle/propeller shocks, could be the source of permanent emission. This possibility was evaluated. Actually, stopping the stirring device did not help acoustic emission to go on, which is not very surprising : given the very high solute concentration involved in this case, it is clear that, due to the high viscosity of the solution, the many shocks occurring in the suspension are strongly damped and can hardly generate waves. Consequently, it is suggested again that the acoustic activity in the frequency domain is due to CA nucleation. This assumption would also explain why the nucleation of CAm (i.e., after time 6000s) gives rise again to a sequence of acoustic activity in the same frequency domain f_1 to f_5. According to the previous assumptions, the disappearance of "high frequency" activity during period γ could be attributed to the fact that the nucleation events are here negligible (i.e. especially during the dissolution of CAa). At the end of period γ, the solute concentration C(t) would thus cross the anhydrous solubility curve and go on decreasing until the final temperature where the solubility of the monohydrated form is finally met, as represented in Fig.3.

Fig.5a displays the pseudo-frequencies of individual acoustic bursts detected by the piezo-sensor. It is interesting to determine to which extent the successive crystallizations of anhydrous and monhydrate CA forms could give rise to specific variations of energy features of the acoustic data. From Fig.5, it appears that the time variations of the AE frequency can roughly be divided into four parts. It should however be noted that, in terms of energy, the observation of dense clouds of (t,*f*) points does not mean that the emission is energetically sustained. In other words, the acoustic activity should also be considered with respect to its energy.

During period β, the thermal signature of the first crystallization (i.e., crystallization of CAa) starting at time $t_1 \cong 3500$ s is significantly shifted with respect to the detection of acoustic bursts. Obviously, from a physical viewpoint, the first nucleation events cannot have any "visible" thermal effect on the reactor content because, due its size, the mass of nuclei is negligible. One can thus conclude that the nucleation of CAa occurs much before time t_1: this is consistent with the hypotheses made above.

During the first "exothermic period", the maximum increase of temperature occurs at $t_3 \approx 4000$s. The temperature trajectory corresponds to the energy released by the growth of anhydrous citric acid which cannot fully be compensated by heat transfer through the jacket wall. As already outlined, the AE sensor detects early acoustic events: when AE occurs, no crystals can visually be observed in suspension and no heat release due to the generation of solid is found to take place. Acoustic events exhibiting frequencies higher than 150 kHz appear to be specific of this period and, consequently, of the generation of CAa.

To get an additional point of view on the crystallization process, a more refined time and frequency domain analysis was performed. The frequency space was shared into the three main domains of interest underlined in Figure 6: [0-150 kHz], [150-300 kHz], and [300-500 kHz]. In order to reduce the amount of acoustic data and to compute a smooth (t, $\bar{f}$, $a\overline{E}_{i,j}$) surface plot, every time domain was divided into 120 s samples. The frequency range was divided into samples of width 4 kHz. The size of the time-frequency grid is therefore [50x70], the frequency and time domains being divided into 50 intervals (300-500 kHz) and 70 intervals (0-8400 seconds), respectively. Thus, the time-frequency domain was cut in 3500 cells.

Every rectangular time-frequency cell (referred below to as [i, j]) is filled by the corresponding absolute energy value computed as follows:

$$a\overline{E}_{i,j} = \frac{\sum_{k=1}^{N_{i,j}} E_k}{\Delta f . \Delta t} \quad (7)$$

where E_k is the value of the absolute energy of hit n°k located inside cell [i, j] and $N_{i,j}$ is the total number of hits inside the same cell, Δf and Δt are the frequency and time intervals defining the size of the [i, j] grid.

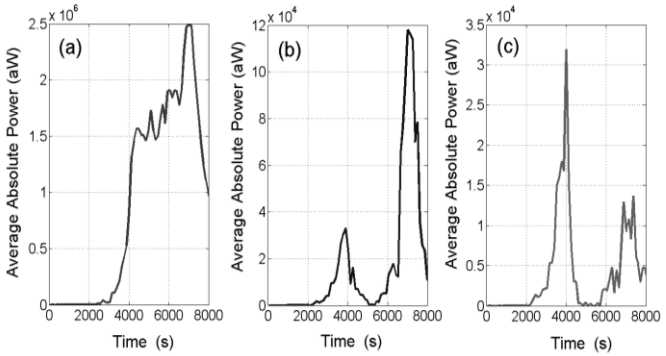

Fig.6. Average integrated absolute energy $\int E_{abs}$ vs. time, measured in 3 frequency domains: (a) [0 150 kHz]; (b) [150 300 kHz]; (c) [300 500 kHz]

To make a deeper analysis of the time/frequency/energy acoustic features during the whole crystallization process, the time variations of the cumulative absolute energy in the frequency bands studied above were computed. Such calculation is represented in the 3 plots displayed in Figure 6. These plots allow a closer look at the variations of the overall average acoustic energy and confirms that the generation of monohydrate can be monitored using on-line AE measurements focused on the frequency bands f_2 to f_5 (i.e., [150-300] kHz.) As one can see in Fig.6b, E_{abs} exhibits two well-separated peaks corresponding to the generation of the two forms of CA during the solvent-mediated phase

transition process. In this frequency area, the second peak is about four times more developed than the peak of anhydrous. This observation suggests that monitoring the appearance of the stable form can be performed through the monitoring of the ratio between the two peaks observed in Fig.6 b & c.

4. A SECOND MODEL SYSTEM: PRECIPITATION OF SALICYLIC ACID THROUGH NEUTRALIZATION.

4.1 Solubility diagram

In this study acoustic emission was recorded during the precipitation of salicylic acid, selected as a second model system. Salicylic Acid (SA) was prepared thanks to the semi-continuous acidification of sodium salicylate solution by sulphuric acid (H_2SO_4). The chemical reaction is:

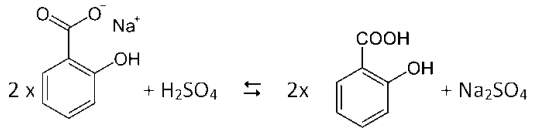

A schematic of the precipitation plant is displayed in Fig. 7. The solution of H_2SO_4 was prepared in reactor n°2 and fed to the solution of sodium salicylate. The concentration of the latter was 0.2 mol/l, it was initially prepared in the glass reactor n°1. Feeding was ensured using a peristaltic pump (Watson 313s). The rate of reaction was therefore controlled by the feeding rate of H_2SO_4. A propeller was used during the whole process for mixing the solution in reactor 1 with a constant stirring rate. The reacting temperature was controlled at a constant setpoint of 20 °C. Reactor 1 was baffled in order to avoid vortex formation.

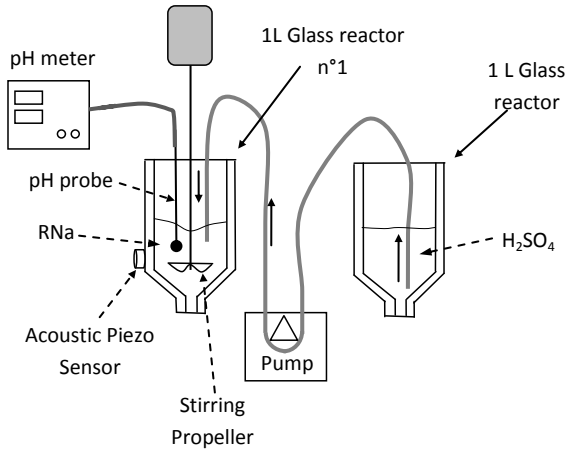

Fig.7. Experimental setup for the semi-continuous precipitation of salicylic acid.

The effect of the feeding rate of H_2SO_4 was investigated: four different input flowrates were applied: [6.4 14 20.8 28] ml/min. The AE monitoring of the experiments was continuous: it started before the beginning of the introduction of H_4SO_4, and was stopped several tenths of minutes after reactor n°2 was emptied. Fig.8 shows that the first AE signals occur significantly later than the beginning of the feeding process. Such delayed onset of the crystallization process was expected because the precipitation process is known to be characterized by a significant supersaturation-dependent induction time (Blandin *et al.*, 2001).

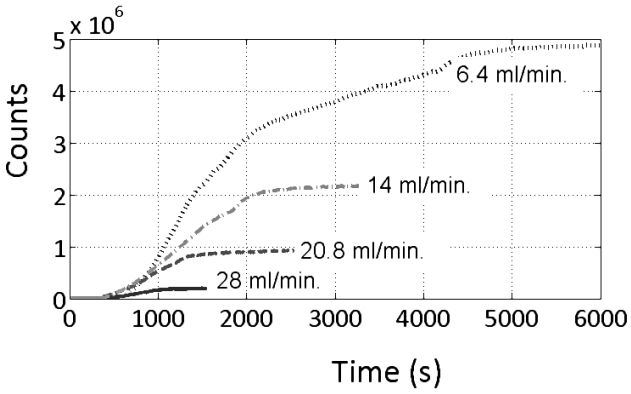

Fig.8. Time evolutions of the number of counts for increasing H_2SO_4 feeding rates.

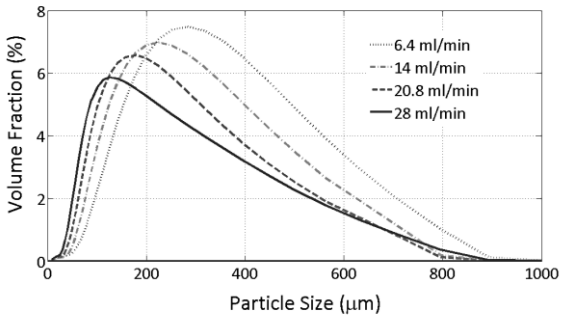

Fig.9. Differential size distributions of SA particles withdrawn at the end of four fed-batch precipitation processes. The measurements were performed off-line.

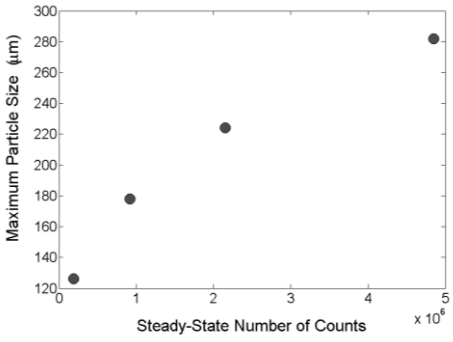

Fig.10. Experimental relationship between the final steady state number of counts and the mode of the corresponding particle size distribution.

Samples of SA suspensions where withdrawn at the end of the batch processes for off-line size measurements. The size analyses were performed using a laser diffraction equipment; the results are displayed in Fig. 9 which shows that increasing cooling rates yield decreasing size distributions. Even though the reproducibility of the AE measurements should be guaranteed before concluding, it appears that there exists some possibility of estimating the mode of the particle size distribution thanks to the monitoring the number of counts recorded at the end of the fed-batch process. Fig. 10 shows that a valuable one-to-one experimental relationship between the steady-state value of the number of counts and

the mode of the crystal size distribution is observed. Should it be confirmed, such result could allow non-intrusive and early estimation of size parameter(s) of particulate products without requiring costly and time-consuming off line size characterizations.

5. CONCLUSIONS.

The present paper shows that several interesting applications regarding the industrial monitoring and control of crystallization processes are made possible by the development of acoustic emission applied as in-line sensing technique. The experimental preliminary results presented here suggest that AE might be valuable for the control of industrial crystallization or precipitation processes as, in addition to its invaluable non-intrusive features, the sensing technique provides many information on both the liquid and the dispersed solid phase evolving in suspension. Among other features, the following attractive potential applications have been suggested in this paper:

- The generation of acoustic signals occurs significantly earlier than the onset of the primary nucleation peak (i.e. before reaching the so-called limit of metastable zone.) Considering that, according to the classical nucleation theory, the latter should not be confused with the first nucleation outbreaks, this fact clearly demonstrates that, more than other usual sensors, AE is undeniably sensitive to basic phenomena arising from the nucleation of the dispersed solid phase.

- The time variations of several descriptors (such as the absolute energy in the case of cooling crystallization of citric acid) can be related to the variation of key fundamental phenomena occurring during batch or fed-batch particulate processes. This was illustrated above through the monitoring of the cooling crystallization of citric acid during which anhydrous to monohydrate phase transition takes place. Considering that polymorphism is a major industrial issue (notable in the field of pharmaceutical processes) this result is quite encouraging.

- In addition to monitoring the development of the crystallization process, it is clearly a very important issue to get in-line estimations of the distribution of particle sizes, the latter being strongly connected to the quality features of the dispersed solid phase. This might allow, for example, to detect off-specification batches much before their termination and, consequently to avoid costly off-line analyses and late rejection of off-specification products. An illustration of this latter potential application of AE was shown with the monitoring of the number of counts during the precipitation of salycilic acid.

6. REFERENCES

Aguiar, P.R., P.J.A. Serni, E.C. Bianchi, F.R.L. Dotto. (2004) In-process grinding monitoring by acoustic emission. In IEEE Int. Conference on Acoustics, Speech, and Signal Processing, 2004. Proceedings. (ICASSP ’04), 5:V405-8 vol.5.

Blandin, A.F., D. Mangin, V. Nallet, J.P. Klein, and J.M. Bossoutrot (2001), « Kinetics identification of salicylic acid precipitation through experiments in a batch stirred vessel and a T-mixer ». Chem. Eng. J. 81 (1-3) 91−100.

Bouchard, J. G., P. A. Payne, et S. Szyszko. (1994), Non-invasive measurement of process states using acoustic emission techniques coupled with advanced signal processing . Chem. Eng. Res. &Des. 72 (A1): 20-25.

B., Javier Villa, C. Sobrino, Jesus Gomez-Hernandez and D. Santana. (2013), Characterization of Flow-Induced Vibrations in Gas-Solid Fluidized Beds: Elements of the Theory. Chemical Engineering Science 93: 181-196.

Burnett, Justin K. (2011), Theory and Uses of Acoustic Emissions. New York: Nova Science Publishers.

Caillet, Al. A. Rivoire, J.M. Galvan, F. Puel, and G. Fevotte. (2007), Crystallization of Monohydrate Citric Acid. 1. In Situ Monitoring through the Joint Use of Raman Spectroscopy and Image Analysis. Cryst. Growth & Design 7 (10): 2080-2087.

Caillet, A., N. Sheibat-Othman, and G. Fevotte. (2007), Crystallization of Monohydrate Citric Acid. 2. Modeling through Population Balance Equations . Crystal Growth & Design 7 (10): 2088-2095.

Févotte, G.. 2002. New perspectives for the on-line monitoring of pharmaceutical crystallization processes using in situ infrared spectroscopy. Int.J.of Pharmaceutics 241 (2): 263-278.

Gherras, N., E. Serris, and G. Fevotte (2012), Monitoring industrial pharmaceutical crystallization processes using acoustic emission in pure and impure media. Int.J. Pharmaceutics 439 (1-2) 109-119.

Grosse, C. U., and Masayasu O. (2008), Acoustic Emission Testing. Springer Verlag.

Jayakumar, T., C.K. Mukhopadhyay, S. Venugopal, S.L. Mannan, and Baldev Raj (2005), A review of the application of acoustic emission techniques for monitoring forming and grinding processes . J. Materials Proc. Technol. 159 (1) 48-61.

Larsen, P. A., and J. B. Rawlings. (2009), The potential of current high-resolution imaging-based particle size distribution measurements for crystallization monitoring . AIChE Journal 55 (4) 896-905.

Naelapää, K., Veski, P., Pedersen, J.G., Anov, D., Jørgensen, P., Kristensen, H.G., Bertelsen, P. 2007. Acoustic monitoring of a fluidized bed coating process . Int.J. of Pharmaceutics 332 (1-2): 90-97.

Nagy, Z. K., and R. D. Braatz. (2012), Advances and New Directions in Crystallization Control . Annual Rev. of Chemical and Biomolecular Engineering 3 (1) 55-75.

Yu, L. X, R.A. Lionberger, A. S. Raw, et al. (2004), Applications of process analytical technology to crystal-lization processes . Adv. Drug Delivery Rev. 56 (3) 349-369.